NANO LETTERS

2007
Vol. 7, No. 2
372−379

Wrinkle-Free Nanomechanical Film: Control and Prevention of Polymer Film Buckling

Troy R. Hendricks and Ilsoon Lee*

Department of Chemical Engineering and Materials Science, Michigan State University, 2527 Engineering, East Lansing, Michigan 48824

Received October 30, 2006; Revised Manuscript Received December 12, 2006

ABSTRACT

For the first time, we report on methods to control and prevent polymer films from buckling. Buckled morphologies were created by thermally cycling or mechanically compressing a poly(dimethylsiloxane) substrate coated with a polyelectrolyte multilayer film. By variation of the dimensions of the surface topography relative to the buckling wavelength (e.g., pattern size is less than, equal to, and greater than the buckling wavelength), the orientation and the local morphology of the buckled films were controlled. On the basis of the information obtained, we demonstrate how to alleviate the unavoidable buckling by incorporating nanoparticles into the film. In addition, we studied the effect of the silica layer that results from oxygen plasma treatment and the critical temperature for permanent film buckling.

Introduction. Buckling or wrinkling is a natural phenomenon which occurs in numerous forms on different length scales.[1] Common forms of buckling include the wrinkling of human skin, the surface of many dried fruits, and even the formation of mountain ranges. Buckling occurs when a film resting on an elastic foundation is compressed. Recently there have been many reports on controlling the buckling morphology of thin metal or silica films on elastic or viscoelastic foundations.[2−7] For many thin film applications buckling can be an undesired result. However none of these buckling studies attempted to prevent buckling from occurring. The prevention of wrinkles caused by aging is of enormous interest to the cosmetics industry.[8] For the first time we studied the control and prevention of buckling in polyelectrolyte multilayer (PEM) films induced by thermal processing or mechanical compression. We demonstrate the ability to control the PEM morphology and have successfully prevented the film from buckling by incorporating nanoparticles into the film.

Polyelectrolyte multilayer coatings can be used on any surface to significantly alter the surface properties.[9,10] Surface modification is done by alternately adsorbing layers of oppositely charged polymers to the surface. The ultrathin polyelectrolyte layers add chemical functionality and change the surface morphology (i.e., thickness, surface roughness, and porosity). The film morphology can be controlled by polyelectrolyte selection, the deposition conditions during assembly (e.g., salt concentration[11−14] and solution pH[11,15]), and the film formation procedure.[11] Rubner and co-workers have shown that for a weak polyelectrolyte system, acid treatment after film formation creates a porous film morphology.[16,17] The film morphology can be cyclically changed from a nonporous to porous state and back, by alternately immersing the films in solutions of moderate and low pH. For practical applications a permanent film morphology and functionality is desired and can be created by cross-linking the PEM thin film coatings.[18] The formation of covalent bonds between the multilayers has been used to create anticorrosion[19] and superhydrophobic surfaces[20] as well as protein-resistant surfaces on poly(dimethylsiloxane) (PDMS).[21] However, a buckled PEM film morphology has not previously been permanently created, spatially controlled, or prevented, by creating compressive forces from the substrate.

Internal compressive stresses caused thermally or mechanically in thin films or their substrates cause the formation of buckles. Buckling has been observed for metal films on top of an elastomeric substrate or film.[3,6,7] A compressive stress is generated by either heating or cooling, this results in the isotropic buckling of the metal film. The generation of a silica layer (up to 500 nm in thickness) on a PDMS substrate and a compressive force, created thermally or mechanically, has also been used to create a buckled surface morphology.[2,4,5] The buckling of multilayered polymer films on stiff substrates due to a change in humidity or temperature has also been demonstrated.[22] A patterned composite PEM film has been shown to buckle in two stages due to adjacent regions having two different Young's moduli.[23] This was done by applying enough compressive force to buckle stiffer

* Corresponding author: e-mail, leeil@egr.msu.edu; phone, (517) 355-9291; fax, (517) 432-1105.

10.1021/nl062544q CCC: $37.00
Published on Web 12/23/2006

regions while the more elastic regions remained unbuckled. When a greater amount of stress is applied, the entire film buckled. The buckling of polymer films has also been used to measure their physical properties.[24,25] This was done at room temperature by applying a reversible external compressive force to the substrate in one dimension that causes the polymer film to buckle in a sinusoidal wave pattern. By measuring the buckling wavelength (λ) and film thickness (d), the Young's modulus (E) of the film can be determined by using

$$\lambda = 2\pi d \left(\frac{E_f(1 - \upsilon_s^2)}{3E_s(1 - \upsilon_f^2)} \right)^{1/3} \quad (1)$$

where ν is the Poisson's ratio and the subscripts s and f refer to the substrate and film, respectively. Further studies have shown that this technique can also be used to find the effective and individual modulus of multiple films composed of more than one material (e.g., polystyrene and PEM) on top of a PDMS substrate.[26,27] The effective modulus is found by treating the multiple layers as one composite film. Of the few studies on polymer films, none of them has shown spatial control over the buckling morphology or attempted to prevent the buckling from occurring.

In our work we present methods to create, spatially control, and prevent permanently buckled PEM films on flat PDMS substrates. The wrinkling is caused by the release of compressive stress created by heating the substrate and allowing it to cool. This thermal cycling can be an irreversible process creating internal stress which induces a permanently buckled morphology.[28] Control over the film buckling morphology is demonstrated by varying the film thickness and the surface topography of the substrate. Additionally the effects of plasma treatment and the critical temperature for permanent buckling are studied. With the knowledge we obtained, the prevention of permanent buckling was demonstrated for the first time, by adding nanoparticles to the films.

Experimental Section. *Materials.* Poly(dimethylsiloxane) (PDMS) was obtained in a Sylgard 184 elastomer kit from Dow Corning (Midland, MI). Poly(allylamine hydrochloride) (PAH, M_w 60 000) and silica nanoparticles (50 ± 10 nm in a 5.65% aqueous solution) were obtained from Polysciences, Inc. (Warrington, PA). Poly(acrylic acid) (PAA, M_w 15 000), poly(diallyldimethylammonium chloride) (PDAC, M_w 100000−200000), and sulfonated polystyrene (SPS, M_w 70 000) were obtained from Sigma-Aldrich (Milwaukee, WI). Deionized (DI) water from a Barnstead Nanopure Diamond (Barnstead International, Dubuque, IA) purification system with a resistance of >18.2 MΩ cm was used for all aqueous solutions. Solution pH was adjusted using 1.0 M HCl or NaOH.

Sample Preparation. Flat PDMS substrates were created by curing the degassed prepolymer and initiator (10:1) mixture against a flat silicon wafer in an oven overnight at 60 °C. The PDMS substrates were plasma cleaned (Harrick Scientific Corporation, Broadway Ossining, NY) with oxygen at ∼0.150 Torr to make their surface hydrophilic. Glass microscope slides (Corning Glass Works, Corning, NY) were sonicated with a Branson ultrasonic cleaner (Branson Ultrasonics Corporation, Danbury, CT) for 20 min in an Alconox (Alconox Inc., New York, NY) solution followed by 10 min of sonication in water. The slides were then blown dry with nitrogen and plasma cleaned with oxygen for 10 min. Silicon wafers were cleaned in piranha solution (7:3 concentrated sulfuric acid; 30% hydrogen peroxide, **CAUTION** *piranha solution reacts violently with organic material, handle with extreme caution*) for 1 h and then plasma treated with oxygen for 4 min. A Carl Zeiss slide stainer was used to deposit PEMs on the plasma-cleaned substrates. The substrates were alternately dipped into a polycationic solution followed by washing in water. The substrate was then dipped into a polyanionic solution followed by washing to create one bilayer. The dipping cycle was repeated to form multilayer films. Two polyion pairs were used, PAH/PAA and PDAC/SPS. The PAH and PAA solutions were 0.01 M (concentration is based on the molecular weight of the polymer repeat unit) and the solution pH was adjusted to 7.5 and 3.5, respectively. The PDAC solution was 0.02 M, and the SPS solution was 0.01 M. Both solutions contained 0.1 M NaCl, and the final solution pH was not adjusted. Multilayer films are abbreviated as $(x/y)_z$ where x is the first polyion deposited, y is the second polyion deposited, and z is the number of bilayers. Half a bilayer means that x was the last polyion deposited.

Thermal Processing. The films were thermally processed by placing PEM-coated substrates in a preheated oven for 2 h. Unless otherwise stated, the oven temperature was set to 180 °C. The samples were removed from the oven and allowed to cool to room temperature on the laboratory bench top.

Silica Nanoparticle Deposition. Polyelectrolyte multilayers were deposited as described above. When a layer of silica nanoparticles was deposited, the samples were removed from the slide stainer and manually drop-coated. Silica nanoparticles were diluted to a 0.5 wt % solution in water. The particles were drop-coated onto the surface for 30 min. Then samples were washed with water and gently blown dry with nitrogen. The slides were then placed back in the slide stainer for adsorption of additional polyelectrolyte layers.

Characterization. Optical microscope images were obtained using a Nikon Eclipse ME600 microscope equipped with a digital camera. Atomic force microscope (AFM) images were collected in tapping mode using a Nanoscope IV multimode scope from Digital Instruments. Root-mean-square (rms) roughness was measured by taking the average of at least seven measurements of a 2.5 μm square box. The buckling wavelength was measured by taking the average of at least seven peak to peak distances of parallel segments. Amplitude was calculated by measuring the height difference between the highest and lowest point of at least seven different line scans and dividing by 2. PEM film thicknesses on silicon and PDMS substrates were measured using spectroscopic ellipsometry on an M-44 ellipsometer (J.A. Woolam Co., Inc.). It has been shown that there is enough

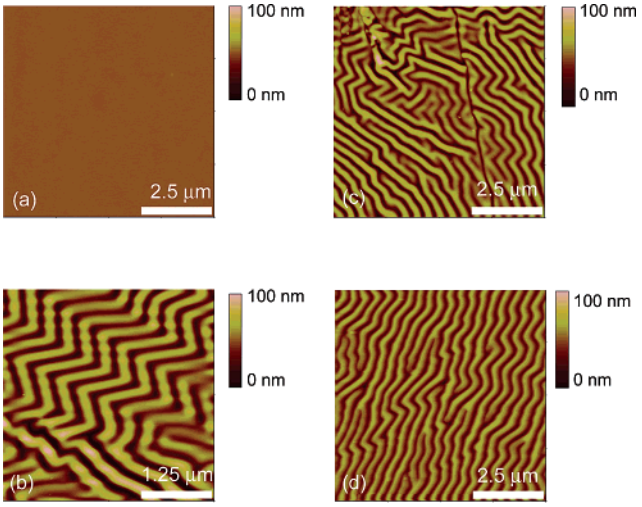

Figure 1. AFM images of flat PDMS substrates after (a) plasma treatment only, (b) plasma treatment and thermal processing the same day, (c) plasma treatment and overnight storage in air followed by thermal processing, and (d) plasma treatment and storage in DI water overnight followed by thermal processing.

contrast in refractive index between PDMS and PEMs to accurately measure the film thickness.[24]

Results and Discussion. *Silica Film Buckling*. The rms roughness of the PDMS substrates was comparable to the roughness of a silicon wafer (<0.5 nm). The repeating unit of PDMS, $-OSi(CH_3)_2-$, creates a hydrophobic surface with an advancing water contact angle of 108°.[29] Treating the surface with oxygen plasma destroys the methyl groups, $Si-CH_3$, and forms a silica layer, SiO_x or Si−OH, which is hydrophilic.[29,30] When plasma-treated PDMS is exposed to air, low molecular weight hydrophobic units ($-CH_3$) migrate to the surface increasing the contact angle. Placing the sample in water after oxidation can retard the regeneration of the hydrophobic surface.[29,30] Previous studies have shown that oxygen plasma treatment and a shift in temperature (either intentional[2] or unintentional[4]) can cause the thin silica layer to buckle. It was not completely clear whether oxygen plasma treatment alone or the combination of plasma treatment and a temperature change would cause the PDMS film to buckle. To investigate whether the wrinkled morphology was caused while the silica layer was being generated, we tested bare PDMS substrates. The thermal processing of pure PDMS did not result in buckling. After a flat PDMS substrate was oxygen plasma treated at room temperature, AFM was used to image the surface. As shown in Figure 1a, a plasma-treated PDMS surface showed no change in surface morphology and had the same rms roughness as an untreated PDMS substrate. Then we thermally processed the plasma-treated PDMS substrates, as illustrated in Scheme 1. These samples include plasma treatment followed by thermal processing in the same day (Figure 1b), plasma treatment followed by storage over night in either air (Figure 1c) or DI water (Figure 1d), and thermal processing the next day. All samples with plasma treatment buckled only after thermal processing. This means both plasma treatment and thermal processing are responsible for the buckling phenomena. The buckling data for oxygen plasma treated PDMS substrates are summarized in Table

Scheme 1. Cross-Sectional Illustration of a Silica Film Generated by Oxygen Plasma Treatment (top) and a PEM Film (bottom) before and after Thermal Processing

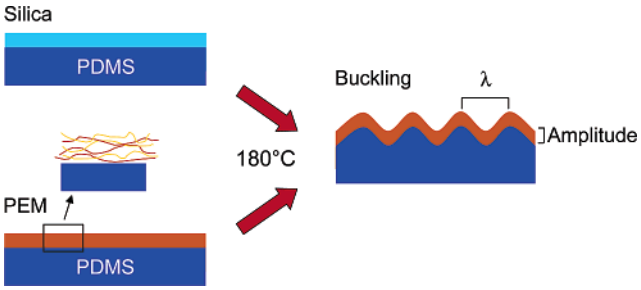

Table 1. Summary of Buckling Data for Oxygen Plasma Treated PDMS Substrates with No PEM Films

additional surface treatment	rms roughness (nm)	wavelength (nm)	amplitude (nm)
none (plasma only)	0.22 ± 0.03		
TP[a] same day	18.9 ± 12.3	386.0 ± 40.2	37.4 ± 6.2
air storage, TP next day	15.0 ± 2.2	453.9 ± 24.5	34.5 ± 7.9
DI storage, TP next day	10.7 ± 0.7	460.8 ± 36.9	18.3 ± 2.5

[a] TP = thermal processing.

1. The sample that was thermally processed the same day as plasma treatment exhibited a smaller wavelength than the samples that were processed the next day. This behavior is caused by a higher Young's modulus due to a shorter time between plasma treatment and thermal processing. Less time between plasma treatment and thermal processing means the surface will have a more silica like layer without the lower modulus hydrophobic material that migrates to the surface over time. The amplitude and wavelength of the buckles in our system are much smaller than a previously demonstrated morphology created with a thermal processing step.[2] Due to the similar refractive indices of the silica layer and PDMS, 1.46 and 1.44, respectively it was not possible to measure the thickness of the silica layer on top of PDMS using an ellipsometer. Instead, we used eq 1 to determine the average thickness for the silica layer. An average silica layer thickness of 3.11 ± 0.3 nm was determined using $\nu_f = 0.33$, $\nu_s = 0.5$, $E_f = 70$ GPa, and $E_s = 1.8$ MPa. This value is lower than expected based on previously reported values.[2,4] We believe that the temperature dependence of the modulus is the cause for our unsatisfactory result.[31] Previous buckling studies with significant temperature shifts were also unsuccessful in calculating the correct modulus when the modulus has previously been determined.[2,3]

Cross-Linkable PEM Film Buckling. Cross-linkable PEM films, $(PAH/PAA)_{5.5}$, were deposited onto flat plasma-treated PDMS substrates. The rms roughness for our PEM film on PDMS measured by AFM is 1.83 ± 0.98 nm. After film formation the samples were thermally processed (see Scheme 1). This type of thermal processing is commonly used to cross-link the PEM films composed of PAH/PAA.[18] When the samples were removed from the oven, the films were optically clear for a couple of minutes. This means there was no necking or crazing that occurred because of the thermal expansion of the PDMS substrate. However, after

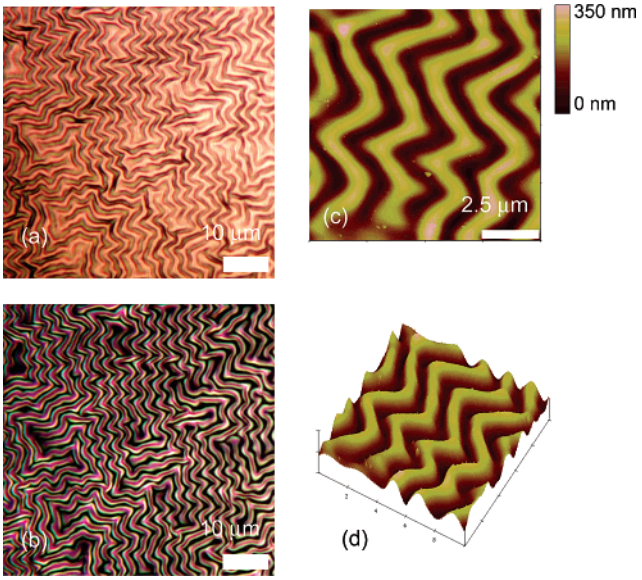

Figure 2. Optical microscope and AFM images of a buckled (PAH/PAA)$_{5.5}$ film on a PDMS substrate after thermal processing: (a) brightfield and (b) darkfield optical microscope images; (c and d) 2D and 3D tapping mode AFM images, respectively. The smooth buckling morphology is caused by a mismatch in thermal expansion between the film and the substrate.

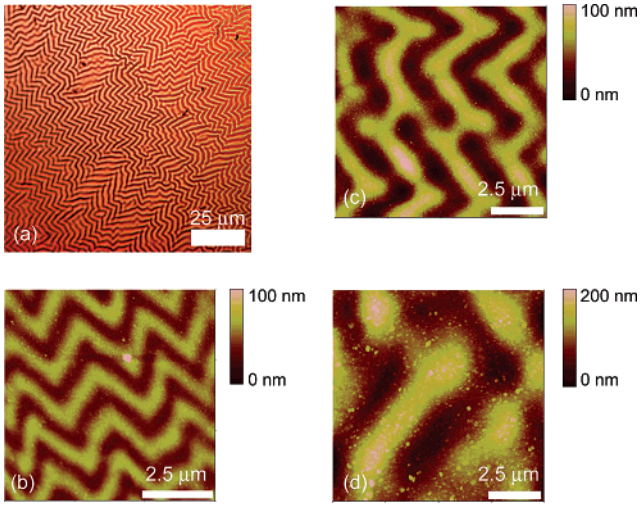

Figure 3. Optical microscope and AFM images of buckled PDAC/SPS films on PDMS substrates after thermal processing. (a) optical microscope image of a (PDAC/SPS)$_{20}$ film; (b−d) tapping mode AFM images of 10, 20, and 40 bilayer PDAC/SPS films respectively. The smooth wavelike morphology is observed again but now for a film that is not known to cross-link.

cooling the samples became translucent indicating a change in the film morphology. Optical microscope and AFM images, shown in Figure 2, confirm the morphology change of these films. The rms roughness of the PEM films increased considerably to 77.43 ± 14.10 nm. For the same films on glass slides there was no morphology change after thermal processing, the PEM film remained optically clear, and the rms roughness did not change. This suggests that the new wavelike morphology was the result of having a PEM film on top of PDMS and not due to the cross-linking of the film. An isotropic biaxial compressive stress was caused by a mismatch in the thermal expansion coefficients between the thin PEM film and the elastomeric PDMS substrate. As the temperature increases from room temperature to 180 °C, the surface area of the PDMS substrate increases ∼20% (using a 3.0×10^{-4} °C^{-1} coefficient of thermal expansion for PDMS).[2] While heated the PEM film may expand with the substrate and rearrange on the PDMS surface. This expansion and rearrangement may cause a reduction in the film thickness along with creating a small number of micrometer-sized cracks in the PEM film where the PDMS surface is exposed. While expanded, no necking or crazing of PEM film was observed. At the elevated temperature of 180 °C, the PAH/PAA film begins to cross-link. As more time passes the film completes cross-linking and becomes more rigid and polyimide-like. When the sample is removed from the oven, the surface area of the PDMS substrate begins to decrease back to its original size at room temperature. Due to the strong adhesion between the rigid PEM film and the PDMS substrate, the film is isotropically compressed and begins to buckle and form the randomly ordered wavelike morphology, as shown in Figure 2. No delamination of the PEM films was observed after heating or cooling. However there was some cracking of the films surface as show in Figure SI 1 of the Supporting Information. This kind of cracking is commonly observed for buckling of thin films.[2,5,23] We theorize that the observed buckling in Figure 2 is the buckling of a two-plate composite film[26] where the silica film and PEM film jointly buckle at the same wavelength. Utilizing eq 1, we calculated an effective modulus of 225 ± 56 MPa for the silica−PEM composite film where $\nu_f = 0.33$, and d is the thickness of the silica−PEM film. This value is significantly lower than the value previously reported for PAH/PAA assembled under the same pH conditions.[26] This happened because eq 1 does not account for the temperature dependence of the Young's modulus.[31] The calculated modulus may also be low because the film thickness may decrease when the PDMS surface expands during the thermal processing.

Non-Cross-Linkable PEM Buckling. To further explore the wrinkling phenomenon, we employed a second PEM film. Non-cross-linkable PDAC/SPS films with different thicknesses were formed on PDMS and thermally processed. Figure 3 shows that the periodic buckling of PDAC/SPS on PDMS does occur for films over a range of thicknesses. Furthermore the buckling is not a result of thermal cross-linking but instead is caused by the difference in coefficients of thermal expansion. The number of bilayers in the PDAC/SPS films was varied to observe the effect of the film thickness on the wrinkled film morphology that is observed after thermal processing. Figure 3 shows AFM images of 10, 20, and 40 bilayer PDAC/SPS films. In agreement with eq 1, the wavelength of the buckles in these films changes linearly with the film thickness. The rms roughness and buckling amplitude also increase linearly with the film thickness. This means that by depositing the appropriate number of polyelectrolyte bilayers onto a PDMS surface, the rms roughness, amplitude, and wavelength of the buckled

Table 2. Summary of Buckling Data for PEM Films on PDMS Substrates

surface	thickness (nm)	rms roughness (nm)	wavelength (μm)	amplitude (nm)
$(PAH7.5/PAA3.5)_{5.5}$	75.4 ± 6.1	77.4 ± 14.1	1.549 ± 0.103	147.4 ± 16.9
$(PDAC/SPS)_{10}$	51.0 ± 7.8	11.7 ± 0.8	0.861 ± 0.840	24.8 ± 3.2
$(PDAC/SPS)_{20}$	98.6 ± 2.0	16.7 ± 2.6	1.976 ± 0.165	40.3 ± 3.5
$(PDAC/SPS)_{40}$	190.2 ± 0.7	24.7 ± 6.3	4.008 ± 0.211	77.8 ± 8.7
$PAH(SPS/PDAC)_{19.5}$[a]	82.1 ± 5.3	127.3 ± 5.0	1.911 ± 0.148	234.6 ± 16.1

[a] Plasma treatment was not used before depositing the PEMs.

film can be controlled. The $(PDAC/SPS)_{20}$ and $(PAH/PAA)_{5.5}$ films have a similar thickness, 98.6 and 75.4 nm, respectively, before thermal processing. However the amplitude of the buckled films is drastically different after the same amount of compressive stress from thermal processing is applied to the samples (see Table 2). The thicker film, $(PDAC/SPS)_{20}$, has a smaller amplitude than the $(PAH/PAA)_{5.5}$ film. This is characteristic of a stiffer (i.e., higher Young's modulus) film. Additionally when eq 1 is used to calculate the effective Young's modulus of the $(PDAC/SPS)_{20}$ film, the result is 208 ± 13 MPa. This value is about the same, within the experimental error, as the effective modulus we calculated for the $(PAH/PAA)_{5.5}$ film but is still 1 order of magnitude lower than values reported for PEM systems.[23,24,26,32] However, the observation that the PDAC/SPS film has a higher modulus than the PAH/PAA film agrees with a report where a PAH/PAA film with more elongated polymer chains, like PDAC/SPS, exhibited a higher modulus than PAH/PAA film with more loopy polymer chains.[32] To further understand the behavior of our system, we manually compressed a $(PDAC/SPS)_{20}$ film and obtained the one-dimensional buckles described previously.[24−27] We determined the buckling wavelength to be 3.26 μm (see Supporting Information Figure SI 2) which is larger than the wavelength produced by thermal processing. Using eq 1, we determined the modulus of a $(PDAC/SPS)_{20}$ film to be 929 ± 57 MPa. This value is slightly less than previously reported values for a $(PAH/SPS)_{20}$ film.[23] We also observed that after compression the PEM film on the pinched sample did not immediately become flat. Buckles on the surface were still observed a half an hour after compression. However after 2 h the sample appeared completely flat under the optical microscope.

Critical Buckling Temperature. The compressive stress, σ, in the PEM film can be calculated as follows[28]

$$\sigma = \frac{E_f(\alpha_s - \alpha_f)}{(1 - \upsilon_f)} \Delta T \tag{2}$$

where α is the coefficient of thermal expansion and ΔT is the difference in maximum and final temperature. The compressive stress is a result of the difference in coefficient of thermal expansion between the film and the substrate.

When the substrates are removed from the oven and the temperature begins to decrease, the PDMS begins to compress the stiff upper film. However the film does not immediately bend until the stress reaches a critical value where the film will finally begin to buckle. This critical stress can be calculated using eq 3.[33,34]

$$\sigma_c = \sqrt[3]{\frac{9}{64} \frac{E_s^{\,2} E_f}{(1 - \nu_s^{\,2})^2 (1 - \nu_f^{\,2})}} \tag{3}$$

The critical compressive stress, σ_c, is dependent on the physical properties (i.e., Young's modulus and Poisson's ratio) of the film and substrate. Once the film buckles, the modulus can be calculated using eq 1. Our system is somewhat more complicated than the one described here since ours is a two-plate composite film.

We experimentally estimated the critical temperature for permanent film buckling of a $(PDAC/SPS)_{20}$ film by changing the maximum temperature of the thermal processing. We tested samples at maximum thermal processing temperatures ranging between 50 and 180 °C. When samples are heated to a maximum temperature of 115 °C, no permanent buckling occurred; however at 120 °C or more, buckling occurred. We determined the critical buckling temperature for permanent film buckling to be ~118 °C. This translates to a critical stress for permanent film buckling of ~3% linear strain for a $(PDAC/SPS)_{20}$ film. We theorize when a PEM film on PDMS is heated to a maximum temperature above 118 °C and then cooled, the process is reversible with no permanent effects on the film morphology (i.e., no permanent buckling). However once the maximum temperature of thermal processing ≥120 °C, the process is irreversible which causes the PEM film to permanently buckle.

Effects of Silica Layer Absence. We further studied the effect of the silica layer created by plasma treatment on the buckling morphology. PDAC/SPS cannot be assembled on a hydrophobic (non-plasma-treated) surface. However by starting with one layer of PAH, at a pH of 7.5, SPS/PDAC can be assembled on PDMS, where PAH interacts with PDMS by hydrophobic interactions and SPS/PDAC can be built on the PAH by electrostatic interactions.[35] We created a 20 bilayer film with a first layer of PAH and 19.5 bilayers of SPS/PDAC, denoted as $PAH(SPS/PDAC)_{19.5}$ in Table 2. This film has a thickness of 81.3 ± 5.3 nm before thermal processing. After thermal processing, the $PAH(SPS/PDAC)_{19.5}$ film buckled as shown in Figure 4. The amplitude of this film is nearly six times larger than that of the $(PDAC/SPS)_{20}$ film. The increase in amplitude is caused by the absence of the silica layer created during plasma treatment that removes a significant amount of the compressive stress

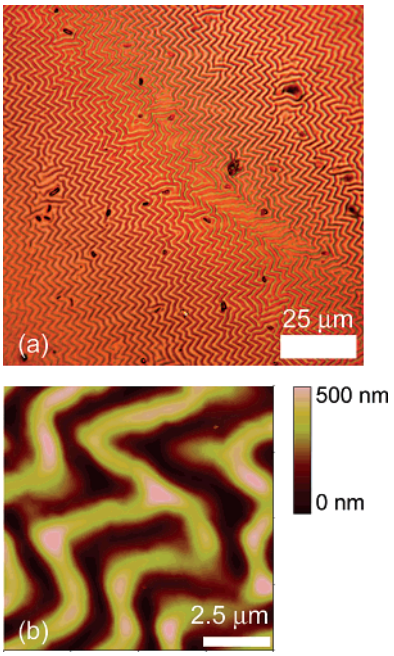

Figure 4. Optical microscope and AFM images of a PAH (SPS/PDAC)$_{19.5}$ film on PDMS with no plasma treatment before multilayer assembly. The amplitude of the waves is high because there is no SiO_2 layer to help absorb the compressive strain.

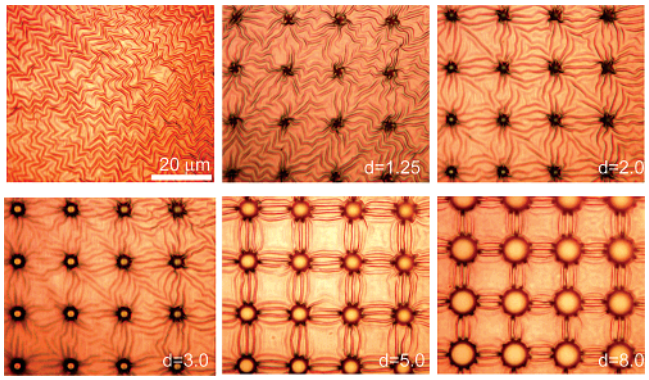

Figure 5. Optical microscope images of a (PAH/PAA)$_{5.5}$ film on a topographically patterned PDMS substrate after thermal processing. The column diameter determines whether the buckled film is ordered ($d > \lambda$) or randomly oriented ($d < \lambda$). The scale bar is valid to all images.

applied to the film from the PDMS substrate. The buckling wavelength does not change much between these two films. This suggests the PAH(SPS/PDAC)$_{19.5}$ film undergoes a different amount of thinning during expansion of the PDMS than a (PDAC/SPS)$_{20}$ film due to the weaker hydrophobic interactions between the PDMS substrate and the PEM films. This difference in expanded film thickness may cause the films to buckle at the same wavelength even though their effective moduli are different.

Surface Topography Effects. The buckled PEM morphology was spatially controlled or prevented by varying the physical topography of the PDMS surface, as shown in Figure 5. We deposited (PAH/PAA)$_{5.5}$ bilayers onto patterned PDMS substrates. The patterned PDMS surfaces contained 2.6 μm high circular columns spaced 18 μm apart (center to center distance) with varying diameters from 1.25 to 9 μm. The PEM-coated PDMS was then thermally processed for 2 h. As shown in Figure 5, the PEM film made a transition from disordered isotropic film buckling (flat PDMS) into a highly ordered buckled morphology (patterned PDMS). This order is caused by the release of the compressive stress in the PEM film at the column.[2,3] The stress is completely released in a direction perpendicular to the columns while the compressive stress in a direction tangent to the column is only partially decreased. This causes the film at the columns to only be compressed in one direction. When compared to the flat PDMS surface, the presence of the 1.25 μm diameter columns increased the wavelength of the PEM film from 1.55 to 2.2 μm due to a reduction in the compressive stress. However, the column diameter is still smaller than the buckling wavelength of the film on a flat surface; hence the buckling is still randomly oriented. Once the column diameter is greater than the flat surface buckling wavelength ($d \geq 2$ μm), the wrinkles begin and end at the columns. At a diameter of 4 μm and above (i.e., larger than the buckling wavelength), the polymer wrinkles only connect to contiguous columns. As the diameter increased further, the number of wrinkles between contiguous columns decreased and the size of the relatively unbuckled region between the columns increased. The presence of surface topography also decreased the number of micrometer-sized cracks in the PEM film. The cracks in homogeneous films reduced the stress and altered orientation of the film buckling similar to changes in the PDMS topography. The area over which the stress was released and the film buckling was affected was ~15 μm for a (PAH/PAA)$_{5.5}$ film (see Supporting Information Figure SI 1).

Prevention of Buckling. Since the buckling of the film due to thermal processing is usually an undesirable result for many thin film applications, for the first time, we set out to prevent the wrinkling from occurring. We observed that physical obstacles (i.e., surface topography) in a film affected the initiation and orientation of the film buckling that occurs around them. On the basis of this fact we hypothesized that the incorporation of nanoparticles may act like a change in the surface topography and perturb the generation of film buckling induced by thermal processing. Our use of PEM films made this a very simple process since the incorporation of functional nanomaterials into a PEM film is widespread.[10] We selectively replaced layers of SPS in a (PDAC/SPS)$_{20}$ film with monolayers of 50 nm negatively charged silica (SiO_2) nanoparticles. As illustrated in Scheme 1, uniform layers on PDMS composed of silica (up to 500 nm), PEMs, or stacked layers of silica and PEMs buckle after thermal processing. The challenge is to integrate silica and PEMs to obtain the physical morphology of a mixed film that does not buckle. To prevent the buckling, first, a single layer of nanoparticles was added at three different positions in the film. The SPS layer in bilayer 1, 10, or 20 was replaced with nanoparticles and thermally processed. The addition of a single layer of nanoparticles, however, did not prevent the film from buckling, possibly due to low nanoparticle surface coverage. The coverage of each layer deposition of silica nanoparticles was not that high due to the electrostatic

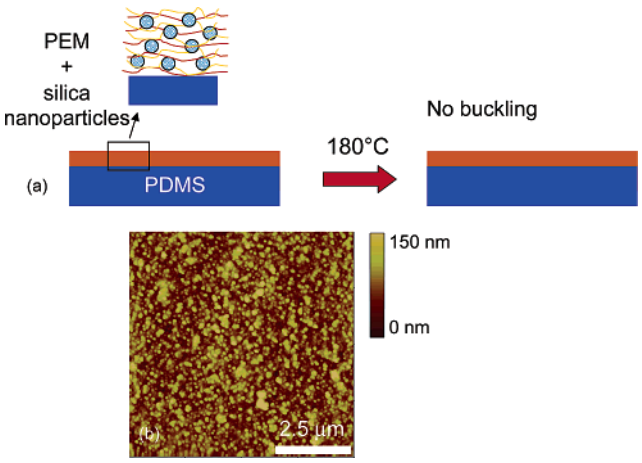

Figure 6. (a) Schematic illustration of the composite nanparticle/polyelectrolyte film, $(PDAC/SiO_2\ (PDAC/SPS)_4)_4$, film before and after thermal processing. (b) AFM image of the film after thermal processing. The addition of nanoparticles alleviates the compressive stress and prevents buckling.

repulsion of the individual nanoparticles. Another film was created where SPS was replaced by SiO_2 nanoparticles in bilayers 1, 6, 11, and 15 abbreviated as $[PDAC/SiO_2(PDAC/SPS)_4]_4$ (illustrated in Figure 6a). An increased number of silica nanoparticle layers within the film resulted in an increase in nanoparticle surface coverage. Due to a small bilayer thickness of ~4 nm, nanoparticles from different depositions were deposited in different nanoscopic planes throughout the entire film. As evidenced in Figure 6b most nanoparticles were evenly distributed in films, but some aggregates were also observed. The thermally processed unbuckled nanocomposite film shown in Figure 6b has an rms roughness of 25.7 ± 1.5 nm. Optical microscope images of the film taken before and after thermal processing show that there is no buckling (see Supporting Information Figure SI 3). Because of the nanometer size of silica particles, the films were still optically transparent. The incorporation of four layers of nanoparticles into the PEM film prevented the film from buckling after thermal processing. According to eqs 2 and 3 adding silica nanoparticles into the film will increase the effective modulus and decrease the critical stress required for buckling. The effective modulus of the mixed films should be between the values of silica and PEM films. Since both homogeneous silica and PEM films buckled, it is very surprising to find that the mixed film did not buckle. We believe the presence of the nanoparticles in the film breakup and alleviate the compressive stress around the nanoparticles in the film so that buckling does not occur. In addition, the buckle-free films were mechanically compressed at room temperature. In a limited region, a small number of buckles were observed propagating from the micrometer-sized cracks. This means that most of the buckling was alleviated or prevented due to the existence of the nanoparticles.

Conclusion. We have shown the creation of buckled PEM films on flat PDMS substrates after thermal processing or mechanical compression. The buckling is caused by the release of compressive stress from the PDMS substrate. The thermally induced stress is created by the significant difference in coefficients of thermal expansion between the PEM film and PDMS substrate. The effect of the silica layer created after plasma treatment has been studied. Control over the film morphology (i.e., buckling) was demonstrated by controlling the film thickness and physical topography of the PDMS substrate. For the first time film buckling was prevented by the addition of silica nanoparticles. We believe this is because the compressive stress, which causes buckling, is decreased (or dissipated) and isotropically dispersed by the nanoparticles in the film. Future studies will include the use of various nanoparticle film compositions (i.e., number of nanoparticle layers and nanoparticle sizes) to prevent the film buckling with less material and/or smaller film thicknesses.

Acknowledgment. We thank the NSF (CTS-0609164) and in part the AFOSR, the Michigan Economic Development Corporation, and the MSU Foundation for their funding of our project.

Supporting Information Available: Optical microscope images of a microcrack in a $(PAH/PAA)_{5.5}$ film, the manually compressed $(PDAC/SPS)_{20}$ film, and a composite nanoparticle/polyelectrolyte film before and after thermal processing. This material is available free of charge via the Internet at http://pubs.acs.org.

References

(1) Genzer, J.; Groenewold, J. *Soft Matter* **2006**, *2*, 310−323.
(2) Bowden, N.; Huck, W. T. S.; Paul, K. E.; Whitesides, G. M. *Appl. Phys. Lett.* **1999**, *75*, 2557−2559.
(3) Bowden, N.; Brittain, S.; Evans, A. G.; Hutchinson, J. W.; Whitesides, G. M. *Nature* **1998**, *393*, 146−149.
(4) Chua, D. B. H.; Ng, H. T.; Li, S. F. Y. *Appl. Phys. Lett.* **2000**, *76*, 721−723.
(5) Efimenko, K.; Rackaitis, M.; Manias, E.; Vaziri, A.; Mahadevan, L.; Genzer, J. *Nat. Mater.* **2005**, *4*, 293−297.
(6) Kim, J.; Lee, H. H. *J. Polym. Sci. Polym. Phys.* **2001**, *39*, 1122−1128.
(7) Yoo, P. J.; Suh, K. Y.; Park, S. Y.; Lee, H. H. *Adv. Mater.* **2002**, *14*, 1383−1387.
(8) Chiu, A.; Kimball, A. B. *Br. J. Dermatol.* **2003**, *149*, 681−691.
(9) Decher, G. *Science* **1997**, *277*, 1232−1237.
(10) Hammond, P. T. *Adv. Mater.* **2004**, *16*, 1271−1293.
(11) Clark, S. L.; Montague, M. F.; Hammond, P. T. *Macromolecules* **1997**, *30*, 7237−7244.
(12) Harris, J. J.; Bruening, M. L. *Langmuir* **2000**, *16*, 2006−2013.
(13) Ladam, G.; Schaad, P.; Voegel, J. C.; Schaaf, P.; Decher, G.; Cuisinier, F. *Langmuir* **2000**, *16*, 1249−1255.
(14) Park, J.; Hammond, P. T. *Macromolecules* **2005**, *38*, 10542−10550.
(15) Shiratori, S. S.; Rubner, M. F. *Macromolecules* **2000**, *33*, 4213−4219.
(16) Hiller, J.; Mendelsohn, J. D.; Rubner, M. F. *Nat. Mater.* **2002**, *1*, 59−63.
(17) Mendelsohn, J. D.; Barrett, C. J.; Chan, V. V.; Pal, A. J.; Mayes, A. M.; Rubner, M. F. *Langmuir* **2000**, *16*, 5017−5023.
(18) Harris, J. J.; DeRose, P. M.; Bruening, M. L. *J. Am. Chem. Soc.* **1999**, *121*, 1978−1979.
(19) Dai, J. H.; Sullivan, D. M.; Bruening, M. L. *Ind. Eng. Chem. Res.* **2000**, *39*, 3528−3535.
(20) Zhai, L.; Cebeci, F. C.; Cohen, R. E.; Rubner, M. F. *Nano Lett.* **2004**, *4*, 1349−1353.
(21) Makamba, H.; Hsieh, Y. Y.; Sung, W. C.; Chen, S. H. *Anal. Chem.* **2005**, *77*, 3971−3978.
(22) Basu, S. K.; Bergstreser, A. M.; Francis, L. F.; Scriven, L. E.; McCormick, A. V. *J. Appl. Phys.* **2005**, *98*, 063507.
(23) Jiang, C.; Singamaneni, S.; Merrick, E.; Tsukruk, V. V. *Nano Lett.* **2006**, *6*, 2254−2259.

(24) Nolte, A. J.; Rubner, M. F.; Cohen, R. E. *Macromolecules* **2005**, *38*, 5367−5370.
(25) Stafford, C. M.; Harrison, C.; Beers, K. L.; Karim, A.; Amis, E. J.; Vanlandingham, M. R.; Kim, H. C.; Volksen, W.; Miller, R. D.; Simonyi, E. E. *Nat. Mater.* **2004**, *3*, 545−550.
(26) Nolte, A. J.; Cohen, R. E.; Rubner, M. F. *Macromolecules* **2006**, *39*, 4841−4847.
(27) Stafford, C. M.; Guo, S.; Harrison, C.; Chiang, M. Y. M. *Rev. Sci. Instrum.* **2005**, *76*, 062207.
(28) Freund, L. B.; Suresh, S. *Thin Film Materials: Stress, Defect Formation of Surface Evolution*; Cambridge University Press: New York, 2003.
(29) Morra, M.; Occhiello, E.; Marola, R.; Garbassi, F.; Humphrey, P.; Johnson, D. *J. Colloid Interface Sci.* **1990**, *137*, 11−24.
(30) Lee, J. N.; Park, C.; Whitesides, G. M. *Anal. Chem.* **2003**, *75*, 6544−6554.
(31) Fujita, H.; Ninomiya, K. *J. Polym. Sci.* **1957**, *24*, 233−260.
(32) Pavoor, P. V.; Bellare, A.; Strom, A.; Yang, D. H.; Cohen, R. E. *Macromolecules* **2004**, *37*, 4865−4871.
(33) Allen, H. G. *Analysis and Design of Structural Sandwich Panels*; 1st ed.; Pergamon Press: New York, 1969.
(34) Volynskii, A. L.; Bazhenov, S.; Lebedeva, O. V.; Bakeev, N. F. *J. Mater. Sci.* **2000**, *35*, 547−554.
(35) Park, J.; Hammond, P. T. *Adv. Mater.* **2004**, *16*, 520−525.

NL062544Q